The Core of Tau-Paired Helical Filaments Studied by Scanning Transmission Electron Microscopy and Limited Proteolysis †

ARTICLE *in* BIOCHEMISTRY · JUNE 2006

Impact Factor: 3.02 · DOI: 10.1021/bi052530j · Source: PubMed

9 AUTHORS, INCLUDING:

Martin Von Bergen
Helmholtz-Zentrum für Umweltforschung
246 PUBLICATIONS **6,021** CITATIONS
SEE PROFILE

Stefan Barghorn
AbbVie
24 PUBLICATIONS **1,805** CITATIONS
SEE PROFILE

Marcus Pickhardt
Deutsches Zentrum für Neurodegenerative E…
37 PUBLICATIONS **1,452** CITATIONS
SEE PROFILE

Ueli Aebi
University of Basel
389 PUBLICATIONS **22,574** CITATIONS
SEE PROFILE

The Core of Tau-Paired Helical Filaments Studied by Scanning Transmission Electron Microscopy and Limited Proteolysis†

Martin von Bergen,*,‡,§ Stefan Barghorn,‡,§,|| Shirley A. Müller,⊥ Marcus Pickhardt,§ Jacek Biernat,§ Eva-Maria Mandelkow,§ Peter Davies,# Ueli Aebi,⊥ and Eckhard Mandelkow*,§

Max Planck Unit for Structural Molecular Biology, Notkestrasse 85, D-22607 Hamburg, Germany, Maurice E. Müller Institute for Structural Biology, Biozentrum, University of Basel, Klingelbergstrasse 70, CH-4056 Basel, Switzerland, and Department of Pathology and Neuroscience, Albert Einstein College of Medicine, 1300 Morris Park Avenue, Bronx, New York 10416

Received December 12, 2005; Revised Manuscript Received January 11, 2006

ABSTRACT: In Alzheimer's disease and frontotemporal dementias the microtubule-associated protein tau forms intracellular paired helical filaments (PHFs). The filaments formed in vivo consist mainly of full-length molecules of the six different isoforms present in adult brain. The substructure of the PHF core is still elusive. Here we applied scanning transmission electron microscopy (STEM) and limited proteolysis to probe the mass distribution of PHFs and their surface exposure. Tau filaments assembled from the three repeat domain have a mass per length (MPL) of ∼60 kDa/nm and filaments from full-length tau (htau40ΔK280 mutant) have ∼160 kDa/nm, compared with ∼130 kDa/nm for PHFs from Alzheimer's brain. Polyanionic cofactors such as heparin accelerate assembly but are not incorporated into PHFs. Limited proteolysis combined with N-terminal sequencing and mass spectrometry of fragments reveals a protease-sensitive N-terminal half and semiresistant PHF core starting in the first repeat and reaching to the C-terminus of tau. Continued proteolysis leads to a fragment starting at the end of the first repeat and ending in the fourth repeat. PHFs from tau isoforms with four repeats revealed an additional cleavage site within the middle of the second repeat. Probing the PHFs with antibodies detecting epitopes either over longer stretches in the C-terminal half of tau or in the fourth repeat revealed that they grow in a polar manner. These data describe the physical parameters of the PHFs and enabled us to build a model of the molecular arrangement within the filamentous structures.

Alzheimer's disease is characterized by the coexistence of two different amyloid deposits in the brain, the extracellular senile plaques composed of fibrils of Aβ peptides and the intracellular paired helical filaments (PHFs)[1] consisting mostly of the microtubule-associated protein tau. Tau is expressed in the adult brain in six isoforms which differ by the presence of two inserts in the N-terminal part (exons 2 and 3) and the second repeat R2 (exon 10) in the repeat domain (Figure 1). The physiological function of tau is to bind and stabilize axonal microtubules. The soluble form of tau has a mostly random coil conformation (*1*, *2*) and thus belongs to the emerging group of natively unfolded proteins (*3*−*5*). Whereas the aggregation of the Aβ peptide can be explained in part by its hydrophobic character, this cannot by applied to tau, which has an overall hydrophilic character and is unusually well soluble. However, tau contains short motifs in the repeat domain which are weakly hydrophobic.

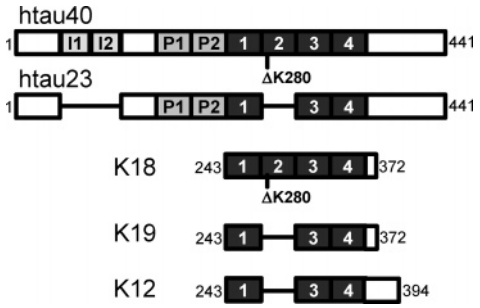

FIGURE 1: Domain composition of tau isoforms and constructs. Top: Htau40 is the largest tau isoform in the human CNS (441 residues). The position of the FTDP-17 deletion mutation ΔK280 is indicated. The C-terminal half contains four pseudorepeats (31 or 32 residues each, R1−R4, in dark gray) which together with their proline-rich flanking regions constitute the microtubule-binding domain. Repeat R2 and the two near N-terminal inserts (I1 and I2, colored in light gray) may be absent due to alternative splicing, as in the smallest (fetal) isoform htau23. Construct K18ΔK280 comprises only the four repeats [residues (M)Q244−E372; 129 residues], construct K19 comprises repeats R1, R3, and R4 as in fetal tau (99 residues), and construct K12 [residues (M)Q244−Y394; 121 residues] comprises three repeats with an additional C-terminal stretch.

† This work was supported by the Deutsche Forschungsgemeinschaft (DFG) and the Swiss National Foundation (NF Grant 3100-059415) and the Maurice E. Müller Foundation of Switzerland.

* Corresponding authors. M.v.B.: tel, +49-40-89982810; fax, +49-40-897168; e-mail, vbergen@mpasmb.desy.de. E.M.: tel, +49-40-89982810; fax, +49-40-897168; e-mail, mand@mpasmb.desy.de.

‡ Both authors contributed equally to this work.

§ Max Planck Unit for Structural Molecular Biology.

|| Present address: Neuroscience Discovery Research, Abbott GmbH & Co. KG, Knollstrasse, 67061 Ludwigshafen, Germany.

⊥ University of Basel.

Albert Einstein College of Medicine.

[1] Abbreviations: AD, Alzheimer's disease; DTT, dithiothreitol; FTDP-17, frontotemporal dementia with Parkinsonism linked to chromosome 17; MPL, mass per length; PBS, phosphate-buffered saline; PHF, paired helical filament; SD, standard deviation; SE, standard error; SELDI-MS, surface-enhanced laser desorption ionization−mass spectrometry; STEM, scanning transmission electron microscopy; TEM, transmission electron microscopy; TFA, trifluoroacetic acid.

10.1021/bi052530j CCC: $33.50
Published on Web 04/27/2006

These hexapeptide motifs in the beginning of the second and the third repeat are crucial for PHF assembly because of their tendency to form β structure (*2*, *6*). The polymerization of tau into PHFs can by facilitated in vitro by polyanions such as heparin, fatty acid micelles, nucleic acids, acidic peptides (poly-Glu), or negatively charged surfaces (*7*−*10*). PHF assembly can be achieved with full-length proteins but is facilitated by removal of the N- and C-terminal domains, indicating that the repeat domain and its flanking regions are largely responsible for the assembly (*11*, *12*).

By negative stain electron microscopy, PHFs from full-length tau and from tau constructs comprising only three or four repeats resemble morphologically those found in Alzheimer's [mostly twisted filaments with somewhat variable crossover repeat, typically ~80 nm (*13*)]. Thus the apparent diameters of the filaments do not reflect the large differences of the protein subunits (more than 4-fold, e.g., 3R tau repeat domain with ~99 residues vs full-length tau with 441 residues). This suggests that only the core of the filaments is revealed with strong contrast by negative stain transmission electron microscopy. A more detailed analysis shows that PHFs from full-length proteins have a "fuzzy coat" outside the core of the filaments (*1*, *14*), whereas PHFs from constructs comprising the repeats show sharper edges (*12*, *15*). The fuzzy coat can be enhanced by special methods such as immunogold labeling or metal shadowing (*16*−*18*).

It is currently unclear whether the protein domains of the fuzzy coat have specific interactions with the PHF core or whether they are projecting from the core in an unspecific manner. Hints to some specific interactions of N-terminal or C-terminal regions with the repeat domain come from conformation-dependent antibodies with discontinuous epitopes which react preferentially with Alzheimer tau. For example, recognition by the antibodies Alz50 and MC1 requires the N-terminus (residues 7−9) and part of the third repeat (313−322) for recognition (*19*−*21*). Similarly, a C-terminal region with amphipathic helix potential (residues 422−438) is thought to fold back onto the repeat domain (*22*). However, the contributions of these conformations to PHF formation are still elusive.

A high-resolution analysis of the entire PHF structure by X-ray crystallography or fiber diffraction will be difficult to achieve because of the largely unfolded nature of tau protein. One therefore has to rely on less direct approaches. Thus, to generate models of the arrangement of tau within the PHFs, the distribution of mass along the filament axis is of importance. This parameter can be analyzed by scanning transmission electron microscopy (STEM). Whereas transmission electron microscopy relies on the staining of the protein by heavy metal salts, STEM is able to visualize the unstained protein and measure the mass per length (MPL) of the structure, taking into account the core as well as the fuzzy coat where present. In earlier studies various samples of filaments from AD brain had been analyzed by EM and STEM (*14*, *23*−*25*), with divergent results that may be related to the type of preparation. The improvements in purification schemes for PHFs from Alzheimer's brain (*26*, *27*) and in the polymerization of recombinant tau prompted us to address once more the issue of mass distribution. In particular, we made use of certain FTDP-17 mutations of tau (e.g., ΔK280) which allow efficient PHF assembly without cofactors, which avoids complications in interpretation.

A second important parameter for models of PHF structure is the surface accessibility of residues. Our earlier spectroscopic studies have shown that repeats R2 and R3 are the most deeply buried in the PHF structure (*28*). However, the positions of surface-exposed loops, which would provide a signature for the course of the polypeptide chain, remained unknown. This issue can be addressed by limited proteolysis. The method has been applied previously to PHFs from Alzheimer's brain in order to define the nature of the core and to reveal protease-sensitive sites (*29*, *30*). We have now performed analogous experiments with PHFs made from pure tau isoforms and constructs. This facilitates the interpretation, compared with the mixture of tau isoforms in AD brain, and reveals that the building principles of AD PHFs are indeed similar to those assembled from recombinant tau in vitro.

MATERIALS AND METHODS

Chemicals and Proteins. Heparin (average molecular mass of 6000 Da) was obtained from Sigma (Steinheim, Germany). Fluorescently labeled heparin (average molecular mass of 18000 Da, fluorescein conjugated) was purchased from Molecular Probes (Eugene, OR). The human tau isoforms (htau40) and tau constructs (K18, K12) (see Figure 1) were expressed in *Escherichia coli* as described (*31*). The numbering of the amino acids is that of the isoform htau40 containing 441 residues (*32*). The protein was expressed and purified as described elsewhere (*33*) making use of the heat stability and FPLC Mono S chromatography with subsequent gel filtration [Superdex 200 for tau isoforms (htau40) and Superdex 75 for tau constructs (K18, K12) (Amersham Biosciences, Freiburg, Germany)]. The purity of the proteins was analyzed by SDS−PAGE. Protein concentrations were determined by the Bradford assay or by UV absorption at 214 nm against a BSA standard curve. The tau mutations were created by site-directed mutagenesis which was performed using the QuikChange site-directed mutagenesis kit (Stratagene, Amsterdam, Netherlands) and the plasmid pNG2 (*33*). Plasmids were sequenced on both strands.

Preparation of Synthetic PHFs. In vitro assembly of PHFs was induced by incubating varying concentrations (typically in the range of 10−50 μM) of mutated tau isoforms (htau40ΔK280) or tau constructs (K18ΔK280) in volumes of 20−500 μL at 37 °C in PBS, pH 7.4 (137 mM NaCl, 3 mM KCl, 10 mM Na_2HPO_4, 2 mM KH_2PO_4), with 1 mM DTT and mixing it with the anionic cofactor heparin (molecular mass ≈ 6000 Da, used at a molar ratio of tau:heparin of 4:1). Preparation of PHFs without the inducing agent heparin (K18ΔK280) followed the same principles as described above but omitting the heparin. PHFs from the construct K12 were also assembled in the absence of inducing agents but using the hanging drop procedure. For this the protein was dialyzed against Tris-HCl, pH 6.8, prior to incubation. The well buffer contained 0.5 M Tris-HCl/1 M sodium acetate, pH 6.8. The protein concentration was 5 mg/mL (382 μM) in 20 μL of 200 mM Tris-HCl/200 mM sodium acetate, pH 6.8. Incubation was carried out at 20 °C for 7 days.

Binding of Fluorescently Labeled Heparin to PHFs. PHF formation was carried out in the presence of fluorescein-labeled heparin with a molar ratio of protein:heparin of 1:0.25 and incubated for 48 h in the case of K19, K18, and

K18ΔK280. Isoforms htau23 and htau40ΔK280 were incubated for 7 days. The reactions were centrifuged at 86000*g* for 1 h; the pellet was washed once with reaction buffer without heparin and centrifuged again. After that, the pellet was dissolved in PBS in the initial volume of the sample, and the fluorescence of the supernatant and pellet was determined.

Fluorescence Spectroscopy. The fluorescence of fluorescein-conjugated heparin was measured in the presence of soluble and aggregated tau using a total volume of 50 μL in a 384-well plate (Cliniplate black from Labsystems, Frankfurt, Germany) in a fluorometer (Safire, Tecan, Maennedorf, Switzerland). Excitation was set at 495 nm and emission at 518 nm, slit widths were both 5 nm, gain was adjusted to 100, and 10 flashes were used per measurement.

Preparation of AD PHFs. Immunoaffinity-purified PHFs were prepared from Alzheimer's disease brains as described previously, using the reaction with the MC-1 antibody (*34*). The Alzheimer PHFs were concentrated by pelleting at 186000*g* for 14 h and resuspended in PBS. The purity of the PHF preparation was analyzed by SDS−PAGE and Western blotting with the rabbit polyclonal pan-tau antibody K9JA (Dako Diagnostics, Hamburg, Germany).

Immunogold Labeling and Transmission Electron Microscopy. For TEM the protein solutions were placed on 600-mesh carbon-coated copper grids for 5 min. The grids were washed twice with PBS−albumin buffer (1%, pH 7.4). For immunogold labeling the grids were incubated on a drop of antibody−gold solution (prediluted 1:50 in PBS) for 1 h in a chamber with a water-saturated atmosphere. After being washed twice with PBS and distilled water the grids were negatively stained with 2% uranyl acetate for 1 min and examined with a Philips CM12 electron microscope at 100 kV. For negative stain electron microscopy 1−10 μM protein solution was stained with uranyl acetate as described above. For colloidal gold−antibody complexes, the colloidal solution was prepared by the reduction of tetrachloroauric acid by sodium citrate (*35*). To form the gold−protein complex 2.5 mL of gold solution and 500 μL of protein solution were mixed and stirred for 15 min. BSA was added to final concentration of 0.1% and stirred for an additional 10 min. The solution was centrifuged at 32000 rpm for 15 min at 4 °C, and the soft pellet was removed carefully.

Scanning Transmission Electron Microscopy (STEM). STEM analysis was performed at the Maurice E. Müller Institute, Biozentrum Basel. PHFs were first concentrated and separated from soluble protein by pelleting them in a benchtop centrifuge at 16000*g* for 20 min at 4 °C and resupended in PBS, pH 7.4, and 1 mM DTT. The protein concentration was adjusted to that required for mass measurements by examining negatively stained samples in a TEM. As soon as the required dilution had been attained, 7 μL aliquots were adsorbed for 1 min to thin carbon films that spanned a thick fenestrated carbon layer covering 200 mesh/in. gold-plated copper grids. The grids were then blotted, washed twice on drops of quartz bidistilled water to remove all buffer salts, immediately frozen in liquid nitrogen, and freeze-dried at −80 °C and 5×10^{-8} Torr overnight in the microscope. A Vacuum Generators STEM HB-5 interfaced to a modular computer system (Tietz Video and Image Processing Systems GmbH, Gauting, Germany) was employed. Details of the instrument's calibration for mass measurements are described elsewhere (*36*, *37*). Dark-field images were recorded from the unstained PHF samples at an accelerating voltage of 80 kV and a nominal magnification of 200000× using electron doses in the range of 350 electrons/nm^2. In addition, repeated low-dose scans were recorded from some grid regions to assess beam-induced mass loss. The 512 × 512 pixel digital images were evaluated using the program package IMPSYS (*37*). In brief, filament segments were defined by square boxes and their course was either automatically tracked or manually defined. The total scattering within an integration box fitted to their width and length was then calculated, and the contribution arising from the carbon support film was deducted. Division by the segment length gave the required mass per length (MPL) value. The mass loss relationships were determined by monitoring the change in filament MPL as the total exposure dose of the repeatedly scanned regions increased. After correction for this effect the full MPL data sets were displayed in histograms and fitted to Gaussian curves. The positions of the MPL peaks, their standard deviations (SD), and an estimate of the number of measurements (*n*) giving rise to them were noted.

Limited Proteolysis. Soluble and polymerized proteins were digested with the endoprotease trypsin (Promega, Madison, WI) at a protein:protease ratio of 500:1 at 37 °C for various times (0, 10, 30, and 60 min). The proteolysis reactions were stopped by addition of one-fifth of the original volume of 5× SDS−PAGE sample buffer. PHFs digested with other proteases such as GluC and chymotrypsin did not yield distinct bands.

SDS−PAGE, Elution, and Blotting. The proteolysis reactions were applied to 4−20% acrylamide Tris−glycine SDS−PAGE (Invitrogen, Carlsbad, CA). Gel electrophoresis was carried out at 200 V and 50 A with constant current. Protein bands were negatively stained with zinc imidazole (*38*) and excised from the gel. The protein was eluted using a Centrilutor electroelution device (Millipore, Bradford, MA). Elution of the proteins was done at 25 mA for 3 h directly into Centricon centrifugal filter devices with an exclusion size of 30 kDa.

Mass Spectrometry. Mass spectrometry was performed with a SELDI-MS instrument (PBSI; Ciphergen, Fremont, CA). Peptides eluted from the gels were dissolved in a saturated matrix solution (sinapinic acid in 50% acetonitrile and 0.5% TFA). The matrix solution was freshly prepared immediately before use. The samples were applied to chips which were covered with a hydrophobic surface (H4 chips; Ciphergen) without any further pretreatment of the target and dried at 37 °C. The measurements were performed in the positive ion mode with various settings of laser power and sensitivity. A mixture of bovine insulin, bovine insulin β chain, ubiquitin, ACTH 18−39 (Sigma, Munich, Germany), and K19 and K18 was used for calibration of the instrument.

N-Terminal Sequencing. Peptides were blotted on PVDF membranes by semidry blotting and briefly stained with Coomassie blue. After destaining with intensive destainer, the bands were cut out. The membranes were completely destained with 0.1% triethylamine in methanol for about 1−3 min. Afterward the membrane pieces were washed twice with 100% methanol for 1 min by vortexing. The membrane

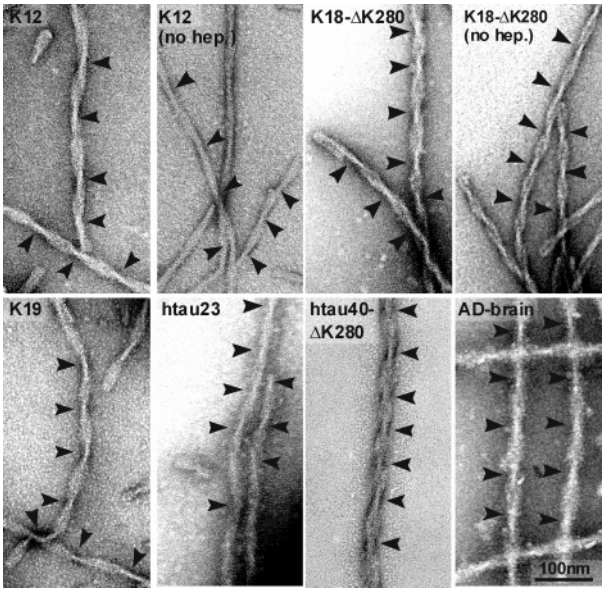

FIGURE 2: Electron micrographs of PHFs. PHFs from Alzheimer's disease brain or assembled from recombinant tau were negatively stained with uranyl acetate and analyzed by transmission electron microscopy. PHFs from K12 or K18ΔK280 were formed with or without heparin, whereas PHF assembly from K19, htau23, and htau40ΔK280 required the presence of heparin. The periodically appearing twists are indictated by arrows.

pieces were dried and used for N-terminal sequencing with a protein sequencer (476A; Applied Biosystems, Foster City, CA).

RESULTS

Proteins and PHF Preparations. To determine the structural parameters of the paired helical filaments, we compared the filaments formed in vivo with those assembled in vitro from recombinantly expressed protein. PHFs from Alzheimer brain are composed of the six isoforms of tau in roughly equal amounts (*39*); they can be purified homogeneously by immunoaffinity chromatography (*19*). PHF assembly from purified tau isoforms in vitro was performed with the longest (htau40) and the shortest isoform (htau23) of tau and with constructs comprising the repeat domain of tau that is involved in microtubule binding (Figure 1). Construct K19 contains the three repeats of ~31 residues each (R1, R3, R4) that are typical of fetal tau, K12 contains the three repeats plus a short C-terminal tail, whereas K18 contains all four repeats (R1−R4). The assembly of tau proteins in vitro is usually stimulated by polyanions in order to achieve reasonable assembly rates, but the mutation ΔK280 observed in FTDP-17 enables efficient assembly even in the absence of polyanions (*40*). This made it possible to examine whether polyanions (such as heparin) are incorporated into PHFs during assembly. Another important aspect for structural studies is the homogeneity of the PHF preparation. Preparations of Alzheimer PHFs based on solubility in sarkosyl (*41*) are more heterogeneous than those prepared by immunoaffinity chromatography (*19*) and PHFs polymerized from pure recombinantly expressed proteins.

Negative Staining Electron Microscopy of PHFs. By negative stain electron microscopy, PHFs assembled in vitro or in vivo typically show a twisted morphology with an axial crossover repeat of ~80 nm (Figure 2). Superficially, the filaments look remarkably similar considering their pronounced differences in composition; for example, K19 contains less than a quarter of the molecular mass of htau40. However, PHFs from the short constructs tend to have sharp edges, whereas PHFs made from full-length tau isoforms or Alzheimer PHFs have fuzzy edges. This reinforces the view that the packing of subunits in PHFs is determined by a core which consists largely of the repeat domain, surrounded by a fuzzy coat (*14*). The poor staining of the fuzzy coat is presumably caused by its loose packing and hydrophilic nature [note that the apparent density of tau is less than that of single-stranded DNA (*11*)]. This makes it difficult to analyze the difference between core and coat by electron microscopy. However, since Alzheimer-like PHFs can be assembled from well-defined recombinant proteins, this issue can be addressed by complementary methods, such as STEM and limited proteolysis, to be described below.

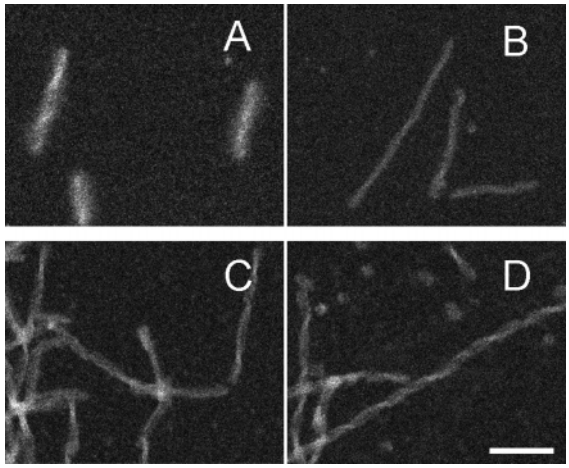

FIGURE 3: STEM analysis. STEM images recorded from unstained samples of (A) htau40ΔK280 PHFs assembled in the presence of heparin, (B) K12 PHFs without heparin, (C) K18ΔK280 PHFs with heparin, and (D) filaments from K18ΔK280 without heparin. The magnification is the same in all micrographs, and the bar in (D) represents 100 nm.

STEM Analysis of the Mass per Length of PHFs. In contrast to negative staining TEM, scanning transmission EM (STEM) is sensitive to the overall mass of the unstained sample and should therefore reveal both the PHF core and the outer coat. Representative examples are shown in Figure 3, and the statistical evaluation is shown in Figure 4. Inspection of the images clearly reveals the fuzzy "halo" around PHFs from full-length tau (Figure 3A), compared to the sharper edges of PHFs from shorter constructs (Figure 3B−D). PHFs from construct K12 (121 residues, 13.08 kDa) polymerized in the absence of heparin show a mass per length (MPL) of 61 ± 9 kDa/nm (Figure 4A). The values are summarized in Table 1 in the Supporting Information. Filaments from the slightly longer construct K18ΔK280 (129 residues, 13.69 kDa) show similar values, 58 ± 6 kDa/nm (assembled with heparin) and 62 ± 5 kDa/nm (without heparin) (Figure 4B,C). The close agreement of these values is remarkable for two reasons. First, they show that similarly sized constructs of the repeat domain assemble with similar packing densities; the observed MPL values are equivalent to 4.3−4.6 molecules of tau/nm. Second, the presence of the polyanionic cofactor (heparin) makes no significant difference to the filament mass. This suggests that the polyanions are incorporated only to a minor extent into the

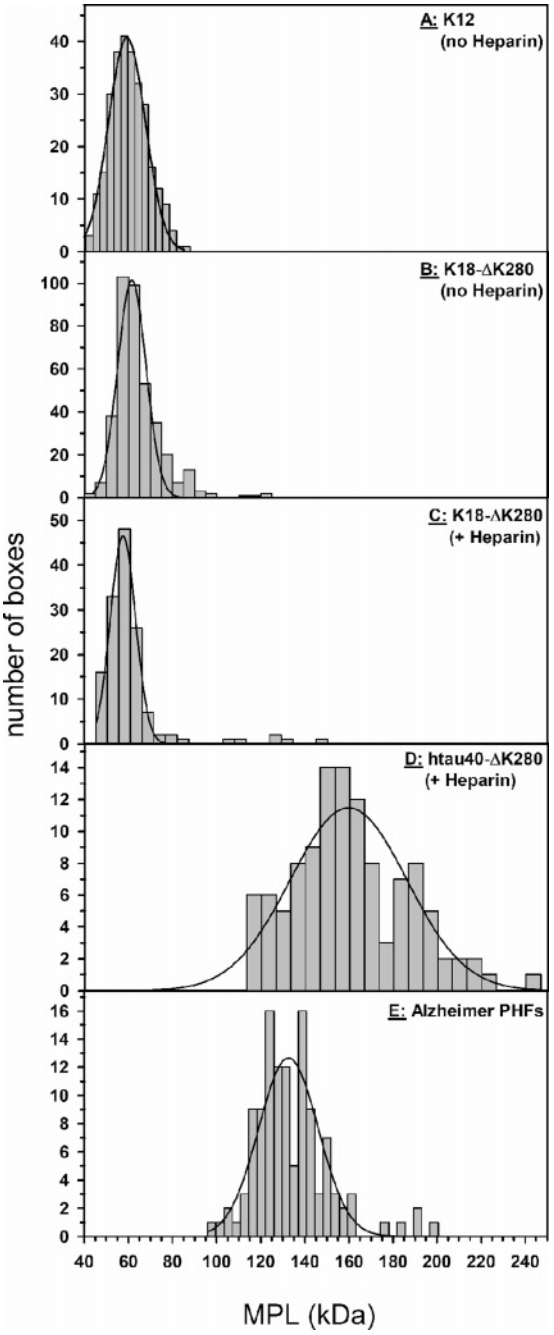

FIGURE 4: Histograms showing the mass-per-length results: (A) K12 without heparin (61 ± 9 nm), (B) K18ΔK280 without heparin (62 ± 5 nm), (C) K18ΔK280 with heparin (58 ± 6 nm), (D) htau40ΔK280 with heparin (157 ± 14 nm), and (E) PHFs from Alzheimer brain (134 ± 14 nm). Data were summarized by plotting mass per length values of >100 individual boxes in histograms. The results were fitted to a Gaussian distribution. MPL values are summarized in Table 1 (see Supporting Information).

filaments, even though they have a major effect on the assembly rate. Given the ratios of molecular mass (K18ΔK280 = 13.69 kDa, heparin = 6 kDa on average) and stoichiometry (4:1 protein:heparin molecule), one would have expected an increase of ~11% in MPL if heparin had been fully incorporated into the PHFs, but this is evidently not the case.

To confirm these findings by an independent method, we tested the incorporation of heparin by using fluorescently labeled heparin for the polymerization of different tau constructs and isoforms (Figure 5). The polymerization reactions were carried out in the standard fashion; subsequently, the PHFs were pelleted, and the fluorescence in the supernatant (gray bars) and pellet (black bars) was analyzed and compared with the initial fluorescence (open bars). The efficiency of polymerization was slightly decreased in comparison to unlabeled heparin. The results show that nearly all of the fluorescence is found in the supernatant, indicating that heparin is not incorporated within the core of the filaments.

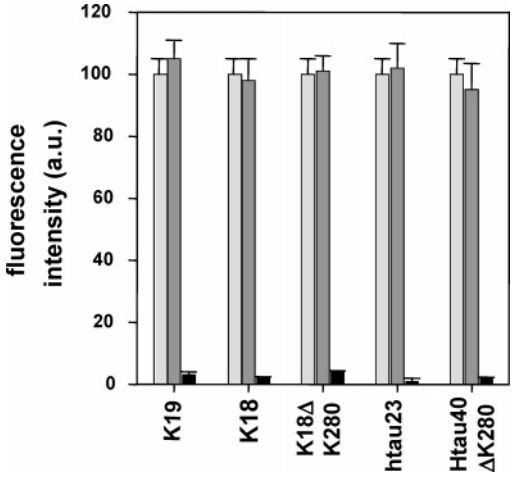

FIGURE 5: PHF assembly with fluorescent heparin. The proteins K19, K18, K18ΔK280, htau23, and htau40 were polymerized in the presence of fluorescently labeled heparin. The fluorescence of the initial reaction mix was measured (gray bars); after polymerization the reaction was centrifuged, and the fluorescence was measured in the supernatant (dark gray bars) and in the pellet fraction (black bars). The fluorescence of the polymerization reaction was set to 100%. Note that almost no heparin is incorporated into the filaments.

PHFs from full-length tau show much larger MPL values, for example, 160 kDa/nm in the case of htau40ΔK280 (440 residues, 45.72 kDa) and 134 kDa/nm for the immunopurified PHFs from Alzheimer brains. The MPL distribution was relatively broad, suggesting a higher degree of heterogeneity (Figure 4D). Given the mass of the full-length htau40, the number of tau molecules per nanometer is 160 kDa nm^{-1}/45.8 kDa $(mol\ of\ tau)^{-1}$ = 3.5 (mol of tau) nm^{-1}. This value is ~30% lower than that observed for the constructs of the repeat domain and indicates that full-length tau is less densely packed than the repeat domain. In the case of Alzheimer PHFs, assuming that the six isoforms of tau occur in roughly equal quantities, their average mass is 41.31 kDa. This translates into 134 kDa nm^{-1}/41.31 kDa $(mol\ of\ tau)^{-1}$ = 3.2 tau molecules/nm. This density of packing is also smaller than that of the repeat domains; however, it is remarkable that it agrees closely with that of the full-length recombinant tau, suggesting that the packing is determined by similar principles in both cases.

Definition of the PHF Core by Limited Proteolysis. The results described so far are consistent with the packing model of core vs fuzzy coat, but they do not reveal where the core begins and ends in the sequence. This question can be addressed by limited proteolysis. A similar approach had been used for Alzheimer PHFs solubilized by formic acid and revealed pronase-resistant fragments of 12 kDa (~100 residues) beginning near the end of R1 (~L266 or H268) or R2 (~I297 or H299) (*30*) (see Figure 7). In this case the protein species was heterogeneous because the PHFs contained a mixture of all tau isoforms. We therefore decided

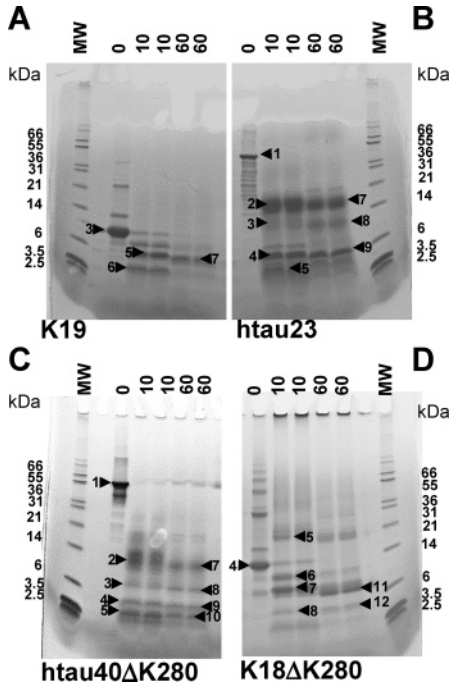

FIGURE 6: Limited digestion of PHFs with trypsin. Products of limited digestion of PHFs from (A) K19, (B) htau23, (C) htau40ΔK280, and (D) K18ΔK280 were applied to Tris−glycine SDS−PAGE and stained by Coomassie blue. Duplicates from two different time points (10 and 60 min) were applied, and the bands which were analyzed are marked by arrowheads. The results of N-terminal sequencing and mass spectroscopy are summarized in Table 2 (see Supporting Information).

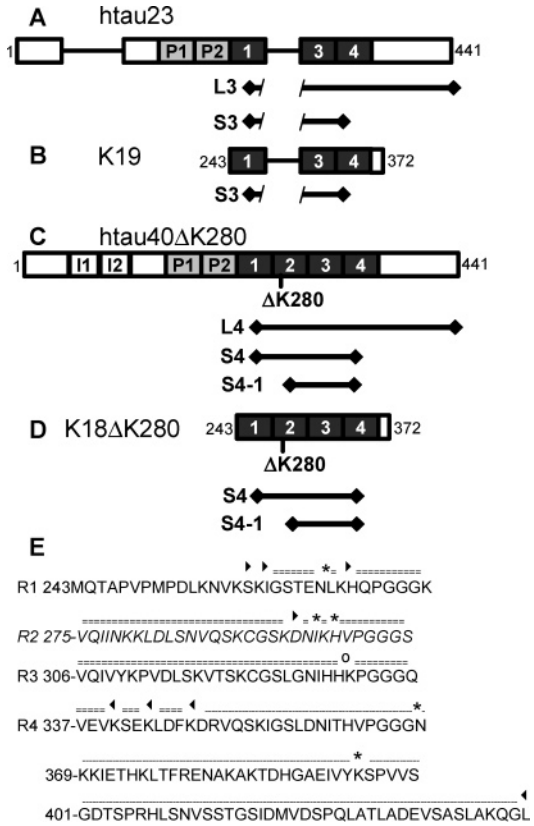

FIGURE 7: Diagram of protease-resistant fragments. Tau proteins and constructs are shown as bar diagrams, and the obtained protease-resistant fragments are shown as lines below in (A) htau23, (B) K19, (C) htau40ΔK280, and (D) K18ΔK280. Please note that there is a common N-terminal end of the protease-resistant core in the first repeat for the three repeat tau proteins, whereas in the case of the four repeat tau proteins there is an additional trypsin cleavage site in the second repeat. The sequence of the repeats is shown in (E). The N-termini of the core fragments are indicated by triangles which point to the right and the C-termini by triangles which point to the left. The cleavage sites found by Jakes et al. (*30*) are marked with asterisks, and the open circles label a lysine in the third repeat which is not cleavable due to the following proline.

to take advantage of the reassembly of homogeneous tau proteins in order to identify accessible cleavage sites in PHFs. As a protease we used mainly trypsin because tau contains numerous target sites (Lys and Arg) so that cleavage is expected wherever the sequence is exposed. Indeed, soluble tau is rapidly and completely degraded by trypsin (not shown), consistent with its natively unfolded structure and the numerous cleavage sites.

PHFs were incubated for 10 or 60 min at a protein:protease ratio of 500:1 and then analyzed by SDS−PAGE, N-terminal sequencing of the excised fragments, and mass spectroscopy. For PHFs made of K19, K18ΔK280, htau23, and htau40-ΔK280, protease-resistant fragments were found even after 60 min of trypsin exposure (Figure 6). The longest protease-resistant band from htau23 PHFs (three repeats) starts in the second half of R1 and ranges up to the C-terminus L441. Sequencing revealed three closely adjacent N-termini, S255, I260, and H268 (Figure 6B, band 2; summarized in Figure 7 and Table 2 in Supporting Information). We refer to this region as trypsin site R1. The persistence of this long fragment extending from site R1 to the C-terminus ("fragment L_3", containing the resistant part of three repeat tau plus the C-tail) means that these domains together are well protected in PHFs (Figure 7A). The second most prominent band (band 4) has the same N-terminus at site R1 (I260, H268) but ranges only to K347 in the middle of the fourth repeat (in the region of site R4; see below), generating a shorter fragment of 80−88 residues in length ("fragment S_3", Figure 7A). Band 3 represents the dimer of band 4. After prolonged proteolysis band 2 was shortened at the N-terminus down to H268 as the predominant N-terminus (Figure 6B, band 7). Band 4 was additionally cut at both ends, yielding band 9 with an N-terminus at H268 and a C-terminus at K347 or K340. The same results were obtained for the dimer of band 9, band 8.

A similar pattern emerged for the digestion of PHFs from the three repeat construct K19 (Figure 6A). Here the largest protease-resistant band starts at the middle of the first repeat (site R1, I260, H268) and ranges to K347 (Figure 6A, band 5), with additional shorter fragments of H268−K343 or H268−K340 terminating in site R4, i.e., 73−88 residues in length (Figure 6A, band 6). After prolonged digestion the most prominent fragment is H268−K340 (Figure 6A, band 7), which appears to arise by cleavage of eight amino acids from the N-terminus and of seven from the C-terminus of band 5 (Figure 6A). Thus, PHFs from three repeat recombinant tau have well-defined borders of protease sensitivity around residues 260−270 and 340−350, generating several variants of fragment S_3 (note that fragment L_3 cannot occur here because K19 extends only to E372).

In the case of PHFs from full-length htau40ΔK280 (four repeats, Figure 6C), the longest stable band (2) starts similarly in the first repeat at site R1 (I260, H268) and extends to the C-terminus of the protein, generating a long resistant fragment L_4 (Figure 7C). The next shorter band (3, Figure

6C) starts at H268 and contains the entire second and third repeat and the beginning of the fourth repeat (up to K347 in site R4), generating the shorter fragment S_4. Further bands (4 and 5, Figure 6C) start in the second repeat at sites D295 or H299 (site R2) that are homologous in position to the cleavage sites in the first repeat (site R1), and they extend to the site R4, the fourth repeat (K340, K347). This generates a shorter version of S_4 termed S_{4-1}. This is analogous to fragment S_3 described above for three repeat tau, except that it begins in repeat 2 and not in repeat 1. After extended digestion band 2 was shortened at the N-terminus by eight amino acids to an N-terminus at H268 (band 7, Figure 6C). After 1 h of proteolysis there was no change of bands 8, 9, and 10, which are identical to bands 3, 4, and 5, respectively. In summary, for PHFs from htau40ΔK280 the N-terminal domain up to the end of the first repeat is initially cleaved off and rapidly digested into small pieces. This is followed by the slower removal of the C-terminal tail, leaving a resistant fragment overlapping largely with the repeat domain. To a lesser extent cleavage inside the second repeat occurs as well so that the core fragments are more heterogeneous than those obtained from the three repeat containing proteins htau23 and K19.

Digestion of PHFs from the four repeat domain construct K18ΔK280 (Figure 6D) yields a similar pattern as the three repeat construct K19. The first resistant bands start at I260 (6) or H268 (7) at site R1 within the first repeat (Figure 6D), both ending at K347 at site R4. In contrast to the full-length protein htau40ΔK280 there is only a minor amount of a band starting within the second repeat (8 in Figure 6D), ranging from D295 (site R2) up to K347 or K340 (site R4). After prolonged digestion, band 7 became slightly shorter at the C-terminus (11, H268−K340, from site R1 to site R4), whereas a fragment which corresponds to band 8 stays the same. In summary, PHFs assembled from the four repeat domain K18 exhibit a similar pattern of protease sensitivity as PHFs from the full-length four repeat protein, namely, an N-terminal region around H268 within the first repeat, a C-terminal region around K343 in the fourth repeat, and an additional cleavage site around H299 in the second repeat. Thus the core peptides are either around 75 residues long, which is equivalent to ∼2.5 repeats (fragment S_4), or alternatively ∼45 residues long (∼1.5 repeats, fragment S_{4-1}).

Immunogold Staining of the PHF Core Defines Structural Polarity. To refine the analysis of the coat−core boundary, we labeled the different types of PHFs with site-specific antibodies and visualized them by immunogold electron microscopy. We used the polyclonal antibody K9JA (raised against construct K9 = Q244−L441, recognizing the whole C-terminal half from the first repeat to the C-terminus) and the monoclonal antibody KBtauR4 [with a clearly defined epitope at L344−Q351 in the fourth repeat (*42*)]. These were labeled with 8 nm gold particles and used as markers of PHF structure.

Since K9JA has a broad epitope distribution which includes the entire core domain, one would expect that it labels PHFs from all protein sources. This was indeed observed, and labeling is seen over the whole length of the filaments (Figure 8A,B; note the example of Figure 8A where the gold particles appear to follow the twist of the PHF, as if labeling occurred only on specific points on the outer surface). In contrast, the epitope of KBtauR4 lies near the

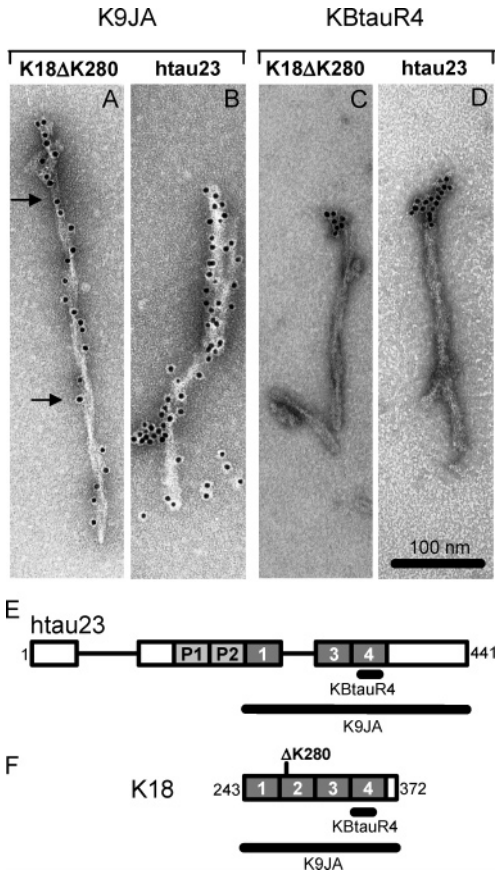

FIGURE 8: Immunogold labeling of PHFs. Electron micrographs of immunogold-labeled and negatively stained PHFs of K18ΔK280 (A and C) and htau23 (B and D) which were decorated with gold particles linked to anti-tau antibodies K9JA (A and B) or KBtauR4 (C and D). The arrows in (A) highlight a region where the gold particles appear to follow the twist of the filament. The bar in panel D represents 100 nm. Panel E illustrates the epitope of the polyclonal antibodies KBtauR4 (restricted to R4) and K9JA (distributed over the repeat domain and the C-terminal tail) in the protein htau23 and (in panel F) the construct K18.

end of the core. Consistent with this, we did not observe labeling along the length of PHFs. However, ends of PHFs were labeled, presumably because the epitope was more exposed. Typically only one of the two ends is labeled, indicating that PHFs have an intrinsic structural polarity (Figure 8C,D).

DISCUSSION

The aim of this study was to contribute to our understanding of the structural principles underlying the pathological aggregation of tau protein into PHFs. It has been known for some time that the aggregation is based on a "core" domain which contains the assembly capacity, surrounded by a fuzzy coat which is poorly visible by TEM (*14*). Isolation of the core by pronase digestion of PHFs revealed that it largely overlapped with the repeat domain of tau and contained well-defined protease-sensitive regions (*29*, *30*). Similar results were obtained with other proteases, e.g., calpain (*43*). However, it remained unclear why tau, a highly soluble protein with hydrophilic character, would form insoluble fibers in aging neurons. Subsequent work, based on recombinant tau, opened up the way to study PHF assembly in vitro (*2*, *7*, *11*, *44*, *45*). It showed that the repeat domain is important for PHF assembly whereas other domains are

inhibitory, that polyanionic cofactors greatly increase the rate of aggregation, and that certain hexapeptide motifs in the repeats are crucial because of their enhanced propensity for β structure. Although the in vitro studies generated filaments resembling bona fide PHFs in terms of overall morphology, the relationship with PHFs formed in cells remained uncertain, partly because a large fraction of the protein in PHFs cannot be visualized reliably, partly because of the unknown effects of the cofactors of assembly on the molecular level, and partly because the folding of the chain in the transition toward PHFs is unknown. This provided the motivation for asking whether the structure and subunit disposition is similar in PHFs from Alzheimer brains and reassembled in vitro, using methods that are sensitive to the mass distribution and surface accessibility such as STEM and limited proteolysis.

STEM Analysis. The STEM results (Figure 4) show that different constructs of the repeat domain with comparable chain lengths (121−129 residues) but differing in composition (e.g., three repeats in K12, four repeats in K18) yield very similar mass per length values, ~60 kDa/nm, corresponding to ~4.3−4.6 molecules/nm. This result argues strongly that the packing is similar, despite the variation in repeat number.

One concern was the contribution of assembly-promoting cofactors such as heparin to the observed mass because this would complicate the interpretation. Unexpectedly, this made no measurable difference, despite its pronounced effect on the rate of PHF assembly. The STEM results were verified biochemically using a fluorescent derivative of heparin, with the same result; i.e., almost none of the heparin coassembled with tau. Thus, heparin plays primarily a kinetic rather than a structural role [note that these results do not confirm the claim that heparin colocalizes with tau fibers in the brain (*7*)]. It is possible that heparin converts soluble tau into a more aggregation-prone conformation [consistent with our recent NMR results (*6*)], and/or that it transiently stabilizes the tau oligomers that nucleate PHFs (*45*). The lack of incorporation of heparin in tau filaments is analogous to the low incorporation of arachidonic acid into tau filaments when the latter is used as an inducer (*10*). In any case, the result means that the STEM data can be interpreted directly in terms of protein distribution.

Full-length tau is ~3.5 times larger than the repeat domain constructs, and therefore, if the packing were identical, one would expect MPL values around 210 kDa/nm for PHFs from full-length tau. The mass distribution shows a shoulder around 180 kDa/nm (Figure 4D), but the bulk of the filaments have lower values around 157 kDa/nm, equivalent to only 3.4 molecules of tau/nm. The reasons for this discrepancy are currently not clear, but it is evident from the distribution that full-length tau PHFs are more heterogeneous and are more loosely packed than those made from the repeat domain. We speculate that the large fraction of the chain outside the repeat domain interferes with the assembly process and thus causes building errors which lead to a suboptimal packing.

This is consistent with the observation that the N- and C-terminal domains tend to slow PHF assembly (*2*, *45*). Here, too, we note that a substantial incorporation of heparin into the filament would not explain the difference either, because this would make the effective mass of the protein even smaller.

By comparison, for PHFs immunopurified from Alzheimer brains we found a mean MPL of 134 kDa/nm. One important difference of these filaments is that they are heterogeneous because they contain all six human tau isoforms in roughly equivalent fractions. Thus, the effective mean mass of the average tau subunit would be around 41 kDa, ~11% less than full-length htau40. On this basis, if the packing were the same as in the htau40-PHFs, one would expect an MPL of 139 kDa/nm, which translates into ~3.4 average molecules/nm on average. Given the uncertainties in the underlying assumptions, we consider the agreement between htau40 PHFs and Alzheimer PHFs rather good, indicating that the packing of subunits is similar in the two cases (and, as mentioned above, allowing for packing defects due to the tau domains outside the core).

How do these values compare with the literature? The problem is that the published values vary over a wide range, and it is evident that this is largely related to differences in preparation. For example, our value of ~134 kDa/nm is in reasonable agreement with the range of 107−120 kDa/nm reported by Kziesak-Reding and co-workers (*25*, *46*). However, the caveat is that our PHFs were immunopurified, whereas earlier preparations relied on different types of solubilization. In addition, the stage of the disease appears to matter, since PHFs from older brains tend to yield lower values, presumably because protein is lost from the fibers due to proteolysis. Thus, tau fibers from Pick's disease were found in a range of 71−113 kDa/nm (*47*), suggesting a packing of about 1.5 tau molecules/nm. Measurements of the pronase-resistant core of AD PHFs yielded about 65 kDa/nm (*14*). This value is in fact in good agreement with the values we obtained from the repeat domain alone (~60 kDa/nm), arguing that the observed packing of the core is similar in both cases, equivalent to ~4−5 tau subunits/nm.

Limited Digestion and Definition of the PHF Core. Limited digestion is a widely used tool to assess the surface exposure of polypeptide chains and to dissect the substructure of proteins and protein assemblies. For choosing a protease as a probing tool, it would be desirable to have a spread of potential cleavage sites on the target protein so that surface-exposed loops can serve as targets. In the case of tau which contains numerous basic residues, trypsin is a natural choice, and in fact all observed cleavage sites occur behind a lysine in the sensitive regions. By comparison, other less specific proteases could also be used [and have been employed to probe the core of AD PHFs (*29*)]. However, we found that this is less suitable for the PHFs assembled from recombinant protein because the protein is digested too quickly and too thoroughly into small pieces, presumably because these PHFs are less stable than AD PHFs and break apart in the process (*28*). On the other hand, chymotrypsin has also been used to identify functional domains in tau protein (*48*), but this protease is not suitable for PHF analysis since tau has only a very low content of aromatic residues.

The results of the limited tryptic digestion of PHFs are remarkably consistent for PHFs made from different forms of tau (full-length or repeat domain).

(1) The N-terminus up to the middle of the first repeat (site R1) is highly sensitive to proteolysis; it is quickly digested into small peptides. This means that the stable core of the PHF starts roughly at site R1 (fragments beginning at

S258, I260, or H268, all consensus sites for tryptic cleavage because of a preceding lysine).

(2) The second-most sensitive site lies in the fourth repeat (site R4, fragments ending at K340, K343, or K347). This implies that the stable PHF core ends at this site. Thus the core comprises roughly the second half of R1, R2 (if present), R3, and the first half of R4.

(3) The C-terminal tail beyond site R4 is semiprotected as long as it is attached to the core, but when cleavage occurs, the C-terminus detaches and is digested quickly into small peptides. This suggests that the C-terminal tail maintains some interaction with the core which tends to protect it (in contrast to the N-terminal domain before site R1 which is not protected).

(4) When R2 is present (as in four repeat forms of tau), there is a secondary cleavage site (site R2, fragments beginning at D295 or H299, both preceded by lysines). This site is located at a position in R2 that is roughly equivalent to site R1 in repeat R1 (allowing for the different locations of cleavable lysines). This suggests that site R2 is in a surface-accessible location, similar to site R1 and site R4.

(5) Thus the resulting fragments may begin either at site R1 or site R2 which differ roughly by one repeat. They may terminate either at site R4 or at the C-terminus, generating "short" or "long" fragments (which differ roughly by 100 residues).

The high proteolytic sensitivity of the N-terminal part of tau was noted previously for soluble tau protein examined by chymotryptic digestion. It allowed an operational distinction between the microtubule-binding "assembly" domain and the nonbinding "projection" domain by cleavage behind Y197 (*48*). The chymotryptic fragments are well detectable because aromatic residues are rare in tau, but here we confirmed the high sensitivity of the N-terminal domain because it is degraded rapidly even at very low enzyme:tau ratios (data not shown). By contrast, the lower proteolytic sensitivity of the C-terminal tail can be explained by an incorporation of the C-terminus into the PHF core structure. For both full-length proteins htau23 and htau40ΔK280 the long fragments appeared at the same rate as the shorter fragments (indicating that the initial cleavage is at site R1). Furthermore, in both cases the longer fragments decreased at the same rate as the shorter ones during prolonged incubation with trypsin. Therefore, the long fragments were not necessarily degraded to the shorter fragments. But, on the other hand, no peptides were detected that comprise the C-terminus without the repeats, arguing that the C-terminus is incorporated within the repeat core, but cleavage within the fourth repeat enables trypsin to degrade the C-terminus completely.

In the soluble state of tau conformationally dependent antibodies indicate an interaction of the C-terminus and the repeat region (antibody MN423 reacts against a truncation site downstream of the repeats at E391) and residues within the repeat domain (*49*) and by indirect approaches measuring the polymerization of tau molecules with and without the C-terminus (*22*). We confirmed an interaction between these regions by FRET of soluble tau with FRET pairs spanning the distance from the repeats to the C-terminus (*50*). These data suggest that already in the soluble tau an interaction is formed, which becomes stabilized after aggregation.

Wischik and colleagues (*29*) showed that AD PHFs can be digested with pronase with little change in the morphology of the filaments. However, the size of the protein subunits was reduced to ~9.5−12 kDa. Further analysis revealed that these fragments consisted of sequences derived from the repeat region and the C-terminal flanking region (*30*). These authors noted the surprising feature that the subunit peptides contained the equivalent of approximately three repeats, yet they originated from both three repeat and four repeat tau. The reason was that cleavage sites occurred both near the end of R1 and near the end of R2 (if present). These sites are in remarkably good agreement with site R1 and site R2 found in our studies. This is strong evidence that the packing of subunits is similar in PHFs from Alzheimer brain and reassembled in vitro, and including different tau isoforms. In all cases there must be exposed loops that are sensitive to proteases (pronase or trypsin) which define the beginning of the protected region of PHFs (Figure 7E). One difference in the two data sets lies in the C-terminus of the protease-resistant core. We found site R4 at the beginning of the fourth repeat (K340−K347), whereas Jakes et al. (*30*) found a chymotryptic peptide with the C-terminus at T384 in a mixture of peptides, obtained from a complete digest of the 12 kDa fragment. The differences in the C-termini between the digestion of AD PHFs of Jakes et al. and this study might be caused by different enzymes that were used or by the different samples. Jakes et al. used PHFs derived from brain, which might be posttranslationally modified, whereas we used highly purified tau protein for assembling PHFs. In immunogold staining experiments the antibody which recognizes the protein when cleaved at E391 labels the fuzzy coat and not the core of the PHFs (*29*), and therefore we assume that the cleavage at the C-terminus by pronase of Alzheimer PHFs might have been influenced by unknown factors.

Some studies have assessed the effect of calpain cleavage of tau (*43*, *51*). Calpain recognizes and cleaves PEST motifs; nine of them were determined in tau (*43*). They are located at positions 11, 44, 230, 254, 257, 267, 310, 340, and 394. PHFs were digested by calpain and the cleavage products analyzed by site-specific antibodies. The authors found that the N-terminal domain was cleaved off up to a position of ~200, whereas the C-terminal domain was not affected. This result is consistent with ours in that it confirms that the N-terminal half of tau in PHFs can be degraded, but the C-terminal half is protected by being part of the core or by close attachment to the core. In recent studies of a cellular model we have shown that aggregation of a four repeat containing fragment of tau (K18ΔK280) was strongly facilitated after cleavage before S258 (*52*).

Immunogold Labeling of the PHF Core. The immunogold labeling data show that the core of the PHFs contains the epitope of an antibody which recognizes a sequence in the beginning of the fourth repeat (KBtauR4). In both full-length isoforms and a shorter fragment comprising only the four repeats, this antibody recognizes only one tip of the polymers. This reveals first that the epitope is not accessible in the core part of the filament and second that it is presented at the two ends of the PHFs differently, indicating a polar structure. It is unclear whether this polar distribution of epitope presentation also means that the growth of PHFs occurs in a polarized fashion as well. A polarity in PHFs is

in good agreement with results from other studies (*53*, *54*). In the case of Aβ a bilateral growth was reported, and similarly for the growth of amyloid fibers from Ure2p, although the elongation rates were different for the two ends (*55*). The recognition of the full length of PHFs by the antibody K9JA, which being a polyclonal antibody has multiple epitopes widely spread over the C-terminal half, shows that the label is tightly attached to the core of the PHFs both in the full-length isoform htau23 and in the four repeat construct K18. These data argue that the C-terminal tail is generally bound to the PHF core; it does not project away from the core and thereby does not contribute much to the fuzzy coat.

Constraints for the Packing of Tau within PHFs. The arrangement of tau in PHFs is unknown, but the data presented here and previously (*2*, *15*, *31*, *56*) provide some important constraints for possible models. The constraints include the following features:

(1) There are roughly 4 tau molecules (range 3.2−4.6) per nanometer of filament length, independent of the tau isoform composition.

(2) The axial repeat is dominated by cross-β structure (*56*, *57*), containing β-strands perpendicular to the filament axis (repeat 0.47 nm, equivalent to ∼2 strands/nm).

(3) The β-strands reside mostly in the repeat domain (around the hexapeptide motifs).

(4) Trypsin-sensitive exposed sites lie in equivalent positions in the repeats, observable in R1 and R2 (not observable in R3, presumably due to the absence of cleavable target motifs).

Figure 9 illustrates one example fulfilling these criteria. Each molecule is shown stretched out across the filament axis; the neighboring one is spaced 0.47 nm above or below to form a β-sheet. This structure amounts to 2 molecules/nm, and therefore two sheets are required to fulfill the STEM criteria (shown as a second sheet, shaded in the background). If we assume that ∼30% of the amino acids are in the β conformation, this would yield 30−40 amino acids in an extended conformation equalling about 11−14 nm (one amino acid = 0.35 nm). This would be in rough agreement with the observed width of the filaments (not considering the residues in the non-β conformation). The orientation of the β-strands could be parallel or antiparallel; the example shows parallel strands within one sheet and antiparallel orientation between the two neighboring sheets, reminiscent of the model of β-amyloid fibrils (*58*).

The protease-sensitive regions are indicated as loops protruding from the sheet structure, located in equivalent regions in 3R or 4R isoforms, as suggested by the tryptic digestion experiments. The observed cleavage sites are indicated by scissors. The cleavage site in repeat R1 represents the beginning of the PHF core and the site in R4 the end of the core. However, in full-length isoforms the C-terminal tail can be tightly associated with the core, as judged by its relative resistance against proteolysis (gray in Figure 9C).

Alternative models can be generated as well, based on similar principles. For example, if each molecule contains a hairpin loop so that two juxtaposed parts of the chain form a cross-β interaction, the height of the molecule would increase to ∼1 nm (2 × 0.47 nm), and therefore four sheets would be required to meet the STEM constraints. Distinguishing between these models will only be possible if further molecular constraints can be introduced, for example, distances between residues derived from X-ray, EPR, NMR, or other types of experiments (see, for example, refs *6*, *56*, and *59*).

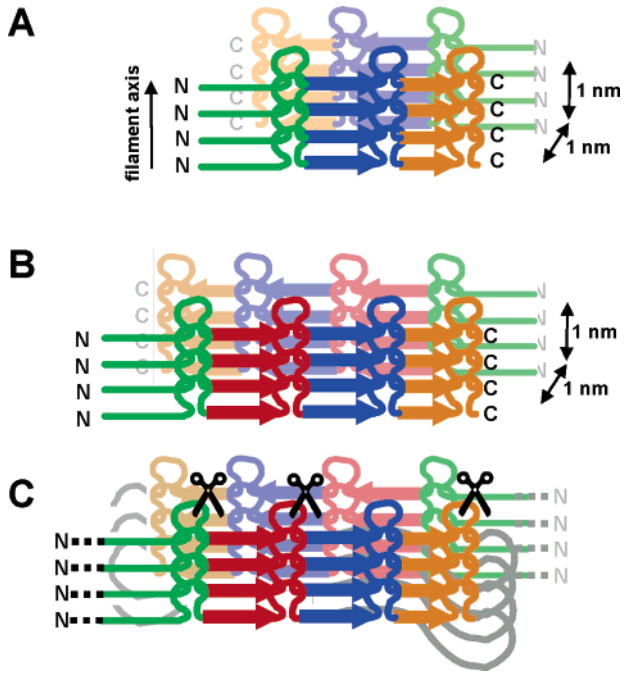

FIGURE 9: Model of the arrangement of tau molecules within the PHFs. Possible arrangements of tau molecules are shown for the construct K19 (A), K18 (B), and htau40 (C). The four repeats are color coded (first repeat in green, second repeat in red, third repeat in blue, and fourth repeat in orange). The filament axis lies in the plane of the paper. The molecules show straight arrows indicating β structure and loops where proteases can cut if a recognition site is present. In the front four molecules form a β-sheet whose strands run perpendicular to the filament axis. Behind it a second sheet in faded colors is shown. The cleavage sites of trypsin are indicated by scissors in (C). The N-terminus (dotted black line) sticks out of the core of the PHFs, whereas the C-terminus (solid gray line) leans against the repeat domain and is partially protected against proteolysis.

ACKNOWLEDGMENT

We thank Bianca Wichmann for excellent technical assistance and Sabrina Hübschmann for help in protein purification and Sabine Wirtz and Vesna Olivieri for the STEM microscopy. We are grateful to Claire Goldsbury for assistance in one of the experiments and Andreas Engel for helpful discussions.

SUPPORTING INFORMATION AVAILABLE

Table 1 summarizing the sample statistics and the results of the STEM analysis and Table 2 summarizing the peptides identified by N-terminal sequencing and mass spectrometry. This material is available free of charge via the Internet at http://pubs.acs.org.

REFERENCES

1. Schweers, O., Schonbrunn-Hanebeck, E., Marx, A., and Mandelkow, E. (1994) Structural studies of tau protein and Alzheimer paired helical filaments show no evidence for beta-structure, *J. Biol. Chem. 269*, 24290−24297.

2. von Bergen, M., Friedhoff, P., Biernat, J., Heberle, J., Mandelkow, E. M., and Mandelkow, E. (2000) Assembly of tau protein into Alzheimer paired helical filaments depends on a local sequence motif ((306)VQIVYK(311)) forming beta structure, *Proc. Natl. Acad. Sci. U.S.A. 97*, 5129−5134.
3. Uversky, V. N. (2002) Natively unfolded proteins: a point where biology waits for physics, *Protein Sci. 11*, 739−756.
4. Dyson, H. J., and Wright, P. E. (2005) Intrinsically unstructured proteins and their functions, *Nat. Rev. Mol. Cell Biol. 6*, 197−208.
5. Dunker, A. K., Lawson, J. D., Brown, C. J., Williams, R. M., Romero, P., Oh, J. S., Oldfield, C. J., Campen, A. M., Ratliff, C. M., Hipps, K. W., Ausio, J., Nissen, M. S., Reeves, R., Kang, C., Kissinger, C. R., Bailey, R. W., Griswold, M. D., Chiu, W., Garner, E. C., and Obradovic, Z. (2001) Intrinsically disordered protein, *J. Mol. Graphics Modell. 19*, 26−59.
6. Mukrasch, M. D., Biernat, J., von Bergen, M., Griesinger, C., Mandelkow, E., and Zweckstetter, M. (2005) Sites of TAU important for aggregation populate beta-structure and bind to microtubules and polyanions, *J. Biol. Chem. 280*, 24978−24986.
7. Goedert, M., Jakes, R., Spillantini, M. G., Hasegawa, M., Smith, M. J., and Crowther, R. A. (1996) Assembly of microtubule-associated protein tau into Alzheimer-like filaments induced by sulphated glycosaminoglycans, *Nature 383*, 550−553.
8. Kampers, T., Friedhoff, P., Biernat, J., and Mandelkow, E. M. (1996) RNA stimulates aggregation of microtubule-associated protein-tau into Alzheimer-like paired helical filaments, *FEBS Lett. 399*, 344−349.
9. Wilson, D. M., and Binder, L. I. (1997) Free fatty acids stimulate the polymerization of tau and amyloid beta peptides. In vitro evidence for a common effector of pathogenesis in Alzheimer's disease, *Am. J. Pathol. 150*, 2181−2195.
10. Chirita, C. N., Necula, M., and Kuret, J. (2003) Anionic micelles and vesicles induce tau fibrillization in vitro, *J. Biol. Chem. 278*, 25644−25650.
11. Wille, H., Drewes, G., Biernat, J., Mandelkow, E. M., and Mandelkow, E. (1992) Alzheimer-like paired helical filaments and antiparallel dimers formed from microtubule-associated protein tau in vitro, *J. Cell Biol. 118*, 573−584.
12. Friedhoff, P., Schneider, A., Mandelkow, E. M., and Mandelkow, E. (1998) Rapid assembly of Alzheimer-like paired helical filaments from microtubule-associated protein tau monitored by fluorescence in solution, *Biochemistry 37*, 10223−10230.
13. Crowther, R. A. (1990) Structural aspects of pathology in Alzheimer's disease, *Biochim. Biophys. Acta 1096*, 1−9.
14. Wischik, C. M., Novak, M., Edwards, P. C., Klug, A., Tichelaar, W., and Crowther, R. A. (1988) Structural characterization of the core of the paired helical filament of Alzheimer disease, *Proc. Natl. Acad. Sci. U.S.A. 85*, 4884−4888.
15. Barghorn, S., Davies, P., and Mandelkow, E. (2004) Tau paired helical filaments from Alzheimer's disease brain and assembled in vitro are based on beta-structure in the core domain, *Biochemistry 43*, 1694−1703.
16. Hasegawa, M., Jakes, R., Crowther, R. A., Lee, V. M., Ihara, Y., and Goedert, M. (1996) Characterization of mAb AP422, a novel phosphorylation-dependent monoclonal antibody against tau protein, *FEBS Lett. 384*, 25−30.
17. Goedert, M., Jakes, R., Crowther, R. A., Cohen, P., Vanmechelen, E., Vandermeeren, M., and Cras, P. (1994) Epitope mapping of monoclonal antibodies to the paired helical filaments of Alzheimer's disease: identification of phosphorylation sites in tau protein, *Biochem. J. 301* (Part 3), 871−877.
18. Ksiezak-Reding, H., Morgan, K., and Dickson, D. W. (1994) Tau immunoreactivity and SDS solubility of two populations of paired helical filaments that differ in morphology, *Brain Res. 649*, 185−196.
19. Jicha, G. A., Bowser, R., Kazam, I. G., and Davies, P. (1997) Alz-50 and MC-1, a new monoclonal antibody raised to paired helical filaments, recognize conformational epitopes on recombinant tau, *J. Neurosci. Res. 48*, 128−132.
20. Jicha, G. A., Weaver, C., Lane, E., Vianna, C., Kress, Y., Rockwood, J., and Davies, P. (1999) cAMP-dependent protein kinase phosphorylations on tau in Alzheimer's disease, *J. Neurosci. 19*, 7486−7494.
21. Carmel, G., Mager, E. M., Binder, L. I., and Kuret, J. (1996) The structural basis of monoclonal-antibody Alz50s selectivity for Alzheimer's-disease pathology, *J. Biol. Chem. 271*, 32789−32795.
22. Abraha, A., Ghoshal, N., Gamblin, T. C., Cryns, V., Berry, R. W., Kuret, J., and Binder, L. I. (2000) C-terminal inhibition of tau assembly in vitro and in Alzheimer's disease, *J. Cell Sci. 113* (Part 21), 3737−3745.
23. Ksiezak-Reding, H., Yang, G., Simon, M., and Wall, J. S. (1998) Assembled tau filaments differ from native paired helical filaments as determined by scanning transmission electron microscopy (STEM), *Brain Res. 814*, 86−98.
24. King, M. E., Ghoshal, N., Wall, J. S., Binder, L. I., and Ksiezak-Reding, H. (2001) Structural analysis of Pick's disease-derived and in vitro-assembled tau filaments, *Am. J. Pathol. 158*, 1481−1490.
25. Ksiezak-Reding, H., and Wall, J. S. (2005) Characterization of paired helical filaments by scanning transmission electron microscopy, *Microsc. Res. Technol. 67*, 126−140.
26. Vincent, I. J., and Davies, P. (1992) A protein kinase associated with paired helical filaments in Alzheimer disease, *Proc. Natl. Acad. Sci. U.S.A. 89*, 2878−2882.
27. Jicha, G. A., O'Donnell, A., Weaver, C., Angeletti, R., and Davies, P. (1999) Hierarchical phosphorylation of recombinant tau by the paired-helical filament-associated protein kinase is dependent on cyclic AMP-dependent protein kinase, *J. Neurochem. 72*, 214−224.
28. Li, L., von Bergen, M., Mandelkow, E. M., and Mandelkow, E. (2002) Structure, stability, and aggregation of paired helical filaments from tau protein and FTDP-17 mutants probed by tryptophan scanning mutagenesis, *J. Biol. Chem. 277*, 41390−41400.
29. Wischik, C. M., Novak, M., Thogersen, H. C., Edwards, P. C., Runswick, M. J., Jakes, R., Walker, J. E., Milstein, C., Roth, M., and Klug, A. (1988) Isolation of a fragment of tau derived from the core of the paired helical filament of Alzheimer disease, *Proc. Natl. Acad. Sci. U.S.A. 85*, 4506−4510.
30. Jakes, R., Novak, M., Davison, M., and Wischik, C. M. (1991) Identification of 3- and 4-repeat tau isoforms within the PHF in Alzheimer's disease, *EMBO J. 10*, 2725−2729.
31. Biernat, J., Mandelkow, E. M., Schröter, C., Lichtenberg-Kraag, B., Steiner, B., Berling, B., Meyer, H. E., Mercken, M., Vandermeeren, A., Goedert, M., and Mandelkow, E. (1992) The switch of tau protein to an Alzheimer-like state includes the phosphorylation of two serine-proline motifs upstream of the microtubule binding region, *EMBO J. 11*, 1593−1597.
32. Goedert, M., Wischik, C., Crowther, R., Walker, J., and Klug, A. (1988) Cloning and sequencing of the cDNA encoding a core protein of the paired helical filament of Alzheimer disease: Identification as the microtubule-associated protein tau, *Proc. Natl. Acad. Sci. U.S.A. 85*, 4051−4055.
33. Gustke, N., Trinczek, B., Biernat, J., Mandelkow, E. M., and Mandelkow, E. (1994) Domains of Tau protein and interactions with microtubules, *Biochemistry 33*, 9511−9522.
34. Jicha, G. A., Berenfeld, B., and Davies, P. (1999) Sequence requirements for formation of conformational variants of tau similar to those found in Alzheimer's disease, *J. Neurosci. Res. 55*, 713−723.
35. Slot, J. W., and Geuze, H. J. (1985) A new method of preparing gold probes for multiple-labeling cytochemistry, *Eur. J. Cell Biol. 38*, 87−93.
36. Engel, A. (1978) Molecular weight determination by scanning transmission electron microscopy, *Ultramicroscopy 3*, 273−281.
37. Muller, S. A., Goldie, K. N., Bürki, R., Häring, R., and Engel, A. (1992) Factors influencing the precision of quantitative scanning transmission electron microscopy, *Ultramicroscopy 46*, 317−334.
38. Scheler, C., Lamer, S., Pan, Z., Li, X. P., Salnikow, J., and Jungblut, P. (1998) Peptide mass fingerprint sequence coverage from differently stained proteins on two-dimensional electrophoresis patterns by matrix assisted laser desorption/ionization-mass spectrometry (MALDI-MS), *Electrophoresis 19*, 918−927.
39. Goedert, M., Spillantini, G., Cairns, N. J., and Crowther, R. A. (1992) Tau proteins of Alzheimer paired helical filaments: Abnormal phosphorylation of all six brain isoforms, *Neuron 8*, 159−168.
40. Barghorn, S., Zheng-Fischhofer, Q., Ackmann, M., Biernat, J., von Bergen, M., and Mandelkow, E. (2000) Structure, microtubule interactions, and paired helical filament aggregation by tau mutants of frontotemporal dementias, *Biochemistry 39*, 11714−11721.
41. Greenberg, S. G., and Davies, P. (1990) A preparation of Alzheimer paired helical filaments that displays distinct tau proteins by polyacrylamide gel electrophoresis, *Proc. Natl. Acad. Sci. U.S.A. 87*, 5827−5831.

42. Ackmann, M., Wiech, H., and Mandelkow, E. (2000) Nonsaturable binding indicates clustering of tau on the microtubule surface in a paired helical filament-like conformation, *J. Biol. Chem. 275*, 30335−30343.
43. Yang, L. S., and Ksiezak-Reding, H. (1995) Calpain-induced proteolysis of normal human tau and tau associated with paired helical filaments, *Eur. J. Biochem. 233*, 9−17.
44. Wilson, D. M., and Binder, L. I. (1995) Polymerization of microtubule-associated protein tau under near-physiological conditions, *J. Biol. Chem. 270*, 24306−24314.
45. Friedhoff, P., von Bergen, M., Mandelkow, E. M., Davies, P., and Mandelkow, E. (1998) A nucleated assembly mechanism of Alzheimer paired helical filaments, *Proc. Natl. Acad. Sci. U.S.A. 95*, 15712−15717.
46. Ksiezak-Reding, H., and Wall, J. S. (1994) Mass and physical dimensions of two distinct populations of paired helical filaments, *Neurobiol. Aging 15*, 11−19.
47. King, M. E., Ghoshal, N., Wall, J. S., Binder, L. I., and Ksiezak-Reding, H. (2001) Structural analysis of Pick's disease-derived and in vitro-assembled tau filaments, *Am. J. Pathol. 158*, 1481−1490.
48. Steiner, B., Mandelkow, E. M., Biernat, J., Gustke, N., Meyer, H. E., Schmidt, B., Mieskes, G., Soling, H. D., Drechsel, D., Kirschner, M. W., et al. (1990) Phosphorylation of microtubule-associated protein tau: identification of the site for Ca(2+)-calmodulin dependent kinase and relationship with tau phosphorylation in Alzheimer tangles, *EMBO J. 9*, 3539−3544.
49. Skrabana, R., Kontsek, P., Mederlyova, A., Iqbal, K., and Novak, M. (2004) Folding of Alzheimer's core PHF subunit revealed by monoclonal antibody 423, *FEBS Lett. 568*, 178−182.
50. Jeganathan, S., von Bergen, M., Brutlach, H., Steinhoff, H.-J., and Mandelkow, E. (2006) Global hairpin folding of tau in solution, *Biochemistry* (in press).
51. Litersky, J. M., and Johnson, G. V. (1992) Phosphorylation by cAMP-dependent protein kinase inhibits the degradation of tau by calpain, *J. Biol. Chem. 267*, 1563−1568.
52. Khlistunova, I., Biernat, J., Wang, Y., Pickhardt, M., von Bergen, M., Gazova, Z., Mandelkow, E., and Mandelkow, E. M. (2005) Inducible expression of tau repeat domain in cell models of tauopathy: Aggregation is toxic to cells but can be reversed by inhibitor drugs, *J. Biol. Chem*. (in press)
53. King, M. E., Ahuja, V., Binder, L. I., and Kuret, J. (1999) Ligand-dependent tau filament formation: implications for Alzheimer's disease progression, *Biochemistry 38*, 14851−14859.
54. Chirita, C. N., and Kuret, J. (2004) Evidence for an intermediate in tau filament formation, *Biochemistry 43*, 1704−1714.
55. Ban, T., Hoshino, M., Takahashi, S., Hamada, D., Hasegawa, K., Naiki, H., and Goto, Y. (2004) Direct observation of Abeta amyloid fibril growth and inhibition, *J. Mol. Biol. 344*, 757−767.
56. Goux, W. J., Kopplin, L., Nguyen, A. D., Leak, K., Rutkofsky, M., Shanmuganandam, V. D., Sharma, D., Inouye, H., and Kirschner, D. A. (2004) The formation of straight and twisted filaments from short tau peptides, *J. Biol. Chem. 279*, 26868−26875.
57. Berriman, J., Serpell, L. C., Oberg, K. A., Fink, A. L., Goedert, M., and Crowther, R. A. (2003) Tau filaments from human brain and from in vitro assembly of recombinant protein show cross-beta structure, *Proc. Natl. Acad. Sci. U.S.A. 100*, 9034−9038.
58. Makin, O. S., and Serpell, L. C. (2005) Structures for amyloid fibrils, *FEBS J. 272*, 5950−5961.
59. Margittai, M., and Langen, R. (2004) Template-assisted filament growth by parallel stacking of tau, *Proc. Natl. Acad. Sci. U.S.A. 101*, 10278−10283.

BI052530J